MARTIN MARIETTA ENERGY SYSTEMS LIBRARIES
3 4456 0361409 7

CENTRAL RESEARCH LIBRARY
DOCUMENT COLLECTION

ORNL-2757
Metallurgy and Ceramics
TID-4500 (14th ed.)

BERYLLIUM THERMAL-CYCLING EXPERIMENT

W. H. Kelley
D. L. Platus
J. R. Tallackson

CENTRAL RESEARCH LIBRARY
DOCUMENT COLLECTION
LIBRARY LOAN COPY
DO NOT TRANSFER TO ANOTHER PERSON
If you wish someone else to see this document, send in name with document and the library will arrange a loan.

OAK RIDGE NATIONAL LABORATORY
operated by
UNION CARBIDE CORPORATION
for the
U.S. ATOMIC ENERGY COMMISSION

Printed in USA. Price 75 cents. Available from the

Office of Technical Services
Department of Commerce
Washington 25, D.C.

LEGAL NOTICE

This report was prepared as an account of Government sponsored work. Neither the United States, nor the Commission, nor any person acting on behalf of the Commission:

A. Makes any warranty or representation, expressed or implied, with respect to the accuracy, completeness, or usefulness of the information contained in this report, or that the use of any information, apparatus, method, or process disclosed in this report may not infringe privately owned rights; or

B. Assumes any liabilities with respect to the use of, or for damages resulting from the use of any information, apparatus, method, or process disclosed in this report.

As used in the above, "person acting on behalf of the Commission" includes any employee or contractor of the Commission, or employee of such contractor, to the extent that such employee or contractor of the Commission, or employee of such contractor prepares, disseminates, or provides access to, any information pursuant to his employment or contract with the Commission, or his employment with such contractor.

ORNL-2757
Metallurgy and Ceramics
TID-4500 (14th ed.)

Contract No. W-7405-eng-26

REACTOR PROJECTS DIVISION

BERYLLIUM THERMAL-CYCLING EXPERIMENT

W. H. Kelley, D. L. Platus, and J. R. Tallackson

DATE ISSUED

SEP 10 1959

OAK RIDGE NATIONAL LABORATORY
Oak Ridge, Tennessee
operated by
UNION CARBIDE CORPORATION
for the
U.S. ATOMIC ENERGY COMMISSION

MARTIN MARIETTA ENERGY SYSTEMS LIBRARIES
3 4456 0361409 7

CONTENTS

Abstract 1

Introduction 1

Design of the Experiment 4

Test Procedure and Test History 7

Test Results 8

Conclusions 10

Appendix A Heat Transfer in Test Piece 12

Appendix B Stress Calculations 15

Appendix C Flow Resistance Calculations 17

References 18

BERYLLIUM THERMAL-CYCLING EXPERIMENT

W. H. Kelley D. L. Platus[1] J. R. Tallackson[2]

ABSTRACT

Severe thermal stresses were anticipated in the beryllium reflector of the Aircraft Reactor Test (ART) and were indicated by approximate calculations. Operation of the ART over any extended period of time would have been accompanied by temperature cycling and, as a consequence, strain cycling. Data on the behavior of beryllium subjected to strain cycling at elevated temperatures are extremely limited, and therefore a reduced-scale experiment designed to test the ART reflector geometry under temperature conditions more extreme than those anticipated in the ART was conducted.

The experiment verified the initial assessment of the situation; the test piece was extensively cracked and the direction and location of the cracks were as expected. A similar set of cracks in the ART reflector would probably not have caused serious trouble, but they might have permitted some of the sodium coolant stream to bypass the lower portion of the reflector and create an undesirable condition.

INTRODUCTION

The reactor designed to be operated as the Aircraft Reactor Test (ART)[3] had a beryllium metal reflector that was pierced with numerous cooling channels. Consideration of the radial temperature gradients in the beryllium reflector indicated the possibility of excessive thermal stresses that would be magnified by the material discontinuities created by the holes for the circulation of the coolant (*1–3*). Since operation of the ART over any extended period of time might have been accompanied by unavoidable temperature cycling and consequent strain cycling at elevated temperatures, it was evident that an accurate assessment of the ability of beryllium to withstand such treatment was needed.

As may be seen from Fig. 1, the most severe radial temperature gradients in the ART reflector would have existed just beneath the load ring. Therefore, this region was considered in making preliminary calculations of thermal stresses in the reflector. The procedure used in calculating the stresses was as follows:

1. The reflector was considered to be a thick-walled, infinite cylinder, and the tangential thermal stresses produced by the gross temperature gradient in a horizontal plane 10 in. above the equator were evaluated (Fig. 2). Appendix A gives details of the method of calculation.
2. The stress-increasing effect of the holes was superimposed on the stresses indicated above. The model used was a hole in an infinite, constant-stress field. When so considered, the stress multiplication (*4*) at the hole boundary is multiplied by a factor of 3. Hole boundary stresses calculated in this manner are given on Fig. 3. It should be noted that the calculated thermal stresses did not include the local stresses around the holes resulting from local temperature gradients produced by coolant (sodium) flow through the holes. These stresses might aggravate the already poor situation.

When allowances are made for the crudity of the calculations and for the assumptions pertaining thereto, it is immediately apparent that the stress values indicated by Fig. 3 are cause for considerable concern. There are no beryllium strain-cycling data directly applicable to this situation;

[1]Now at the University of California at Los Angeles.

[2]Now a member of the ORNL Instrumentation and Controls Division.

[3]Design work on the ART was terminated in the fall of 1957, but some basic work of the type described here was continued because of the applicability of the information in other systems.

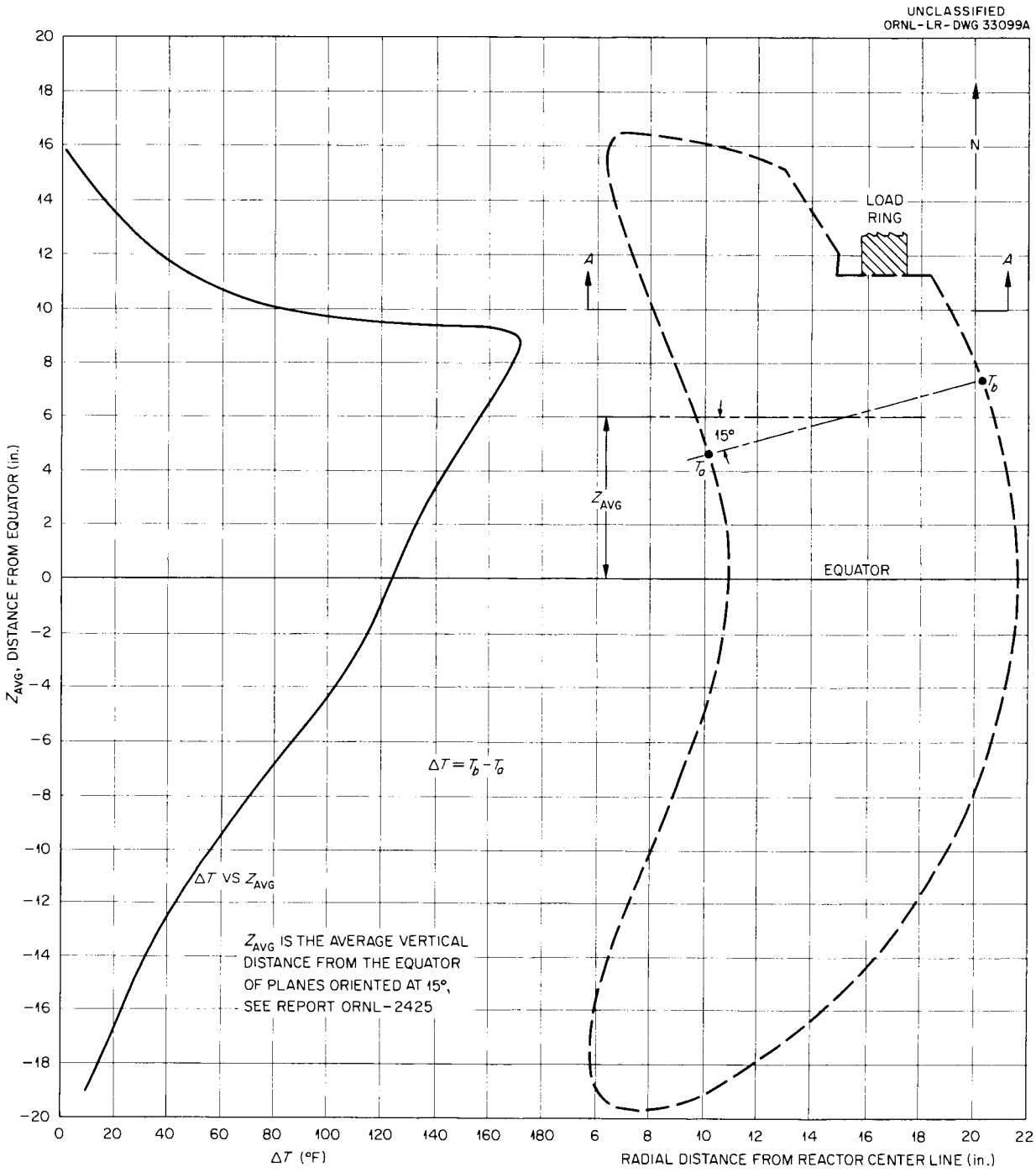

Fig. 1. Radial Temperature Gradient in the ART Reflector [See Ref (2)].

however, reactor-grade QMV beryllium containing approximately 1% BeO displays a yield strength of about 10,000 psi at 1200° F for low strain rates (5). A typical stress-rupture curve (5) at 1200° F shows times to rupture of 2 hr at stresses in the region of 5000 psi. It may be concluded that thermal stresses of the order of 84,000 psi (Fig. 3) will cause either immediate fracture or plastic flow with subsequent stress reversal upon restoration of isothermal conditions in the beryllium. Plastic flow is the more probable and at these stress levels would result in eventual failure.

UNCLASSIFIED
ORNL-LR-DWG 38076A

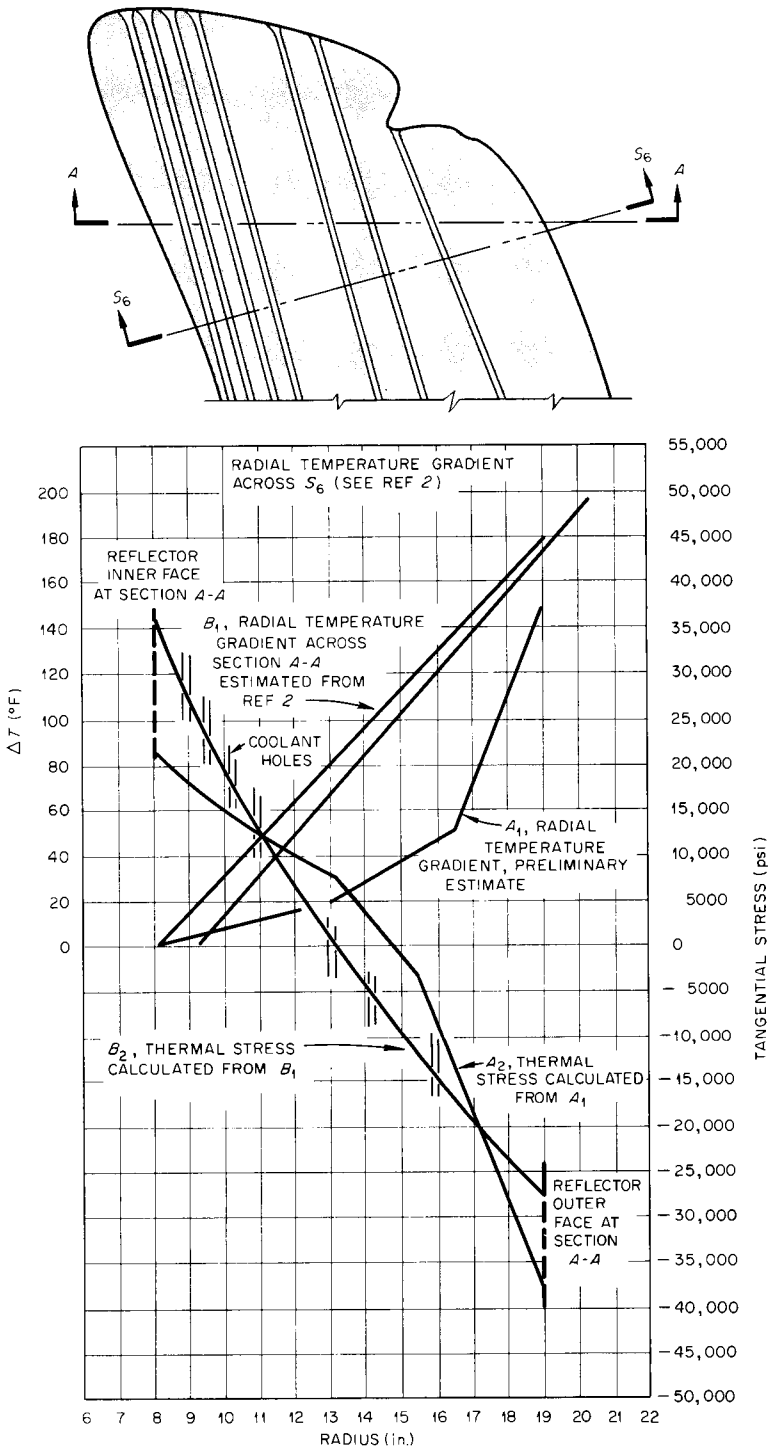

Fig. 2. Tangential Thermal Stresses Produced by the Gross Temperature Gradient in a Horizontal Plane 10 in. Above the Equator.

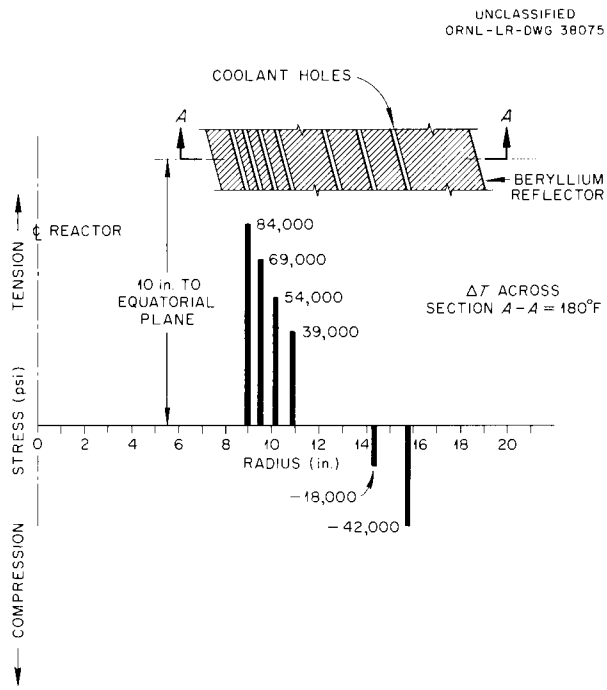

Fig. 3. Estimated Tangential Stress Concentrations at Coolant Holes in Reflector at Horizontal Section *A-A*.

Therefore, it was decided to investigate the behavior of a beryllium sample having similar geometry, including stress-increasing holes, when subjected to temperature cycling at the temperature levels expected in the ART. The temperature differential used in the test was arbitrarily set at 350° F, a figure greater than the temperature differential across the reflector. This first test was essentially an effort to bracket the region in which thermal stress cycling could be expected to produce failures and to serve as a guide to future work; as such, the stress values were not directly applicable to design. For economy, the test was not set up to determine the exact number of cycles to failure.

DESIGN OF THE EXPERIMENT

The simplest approach to simulating the thermal stresses in the reflector was to subject a thick-walled hollow cylinder with holes in the wall to cyclic temperature gradients which would produce comparable stresses at the temperature levels of the reflector. The test piece and its housing are shown schematically in Fig. 4. The small, $\frac{1}{16}$-

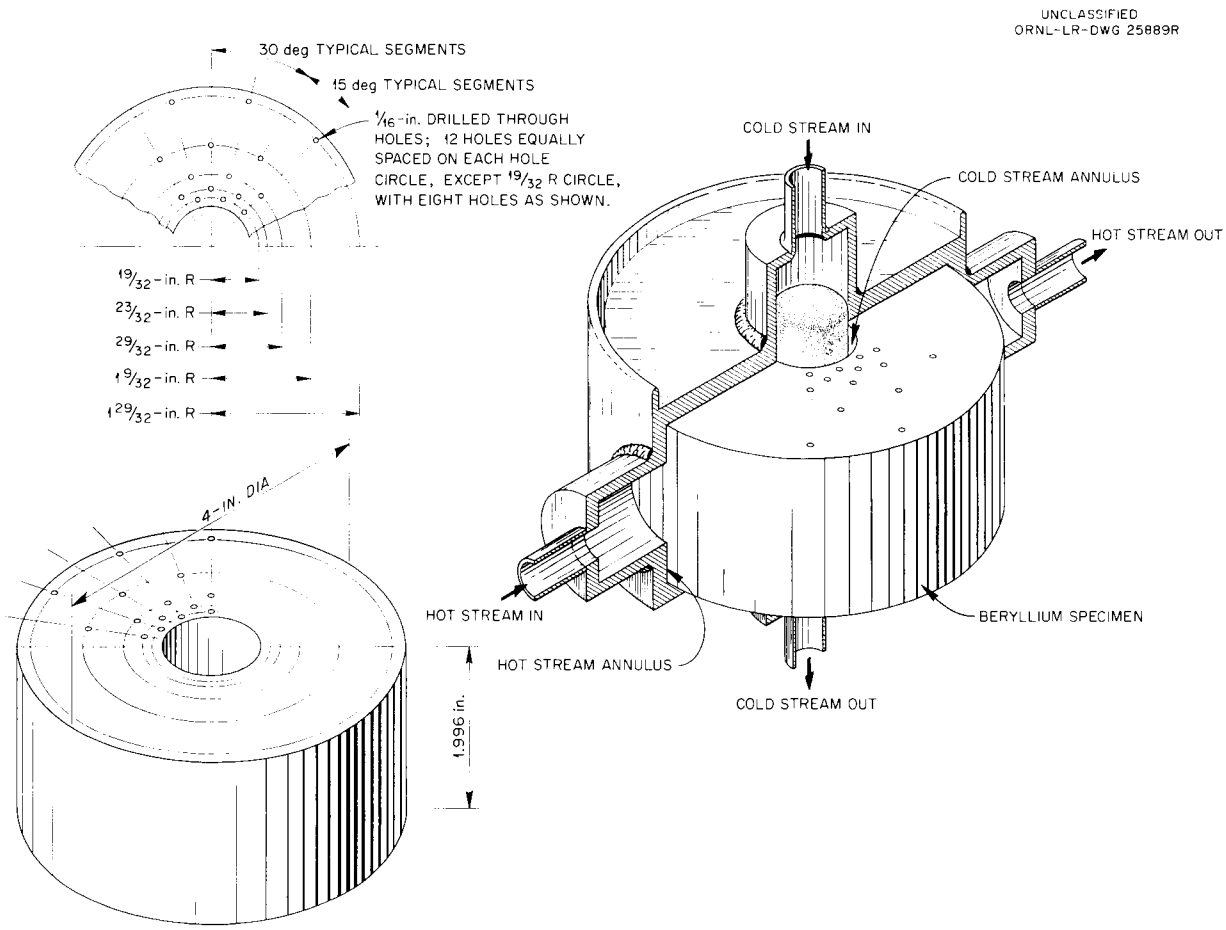

Fig. 4. Test Piece and Housing for Beryllium Thermal-Cycling Test.

in.-dia holes simulate the coolant holes in the reflector and are geometrically similar in size and location.

Appendix B gives details of the stress and heat transfer calculations which established the test conditions. A plot is presented in Fig. 5 of tangential thermal stresses in a cylinder with a concentric hole and with the temperature difference between the inner surface and the outer surface as a parameter. The maximum hole boundary stresses at the $\frac{1}{16}$-in.-dia holes in the test piece that were obtained by using a stress-concentration factor of 3, as in Fig. 3, are given in Fig. 6.

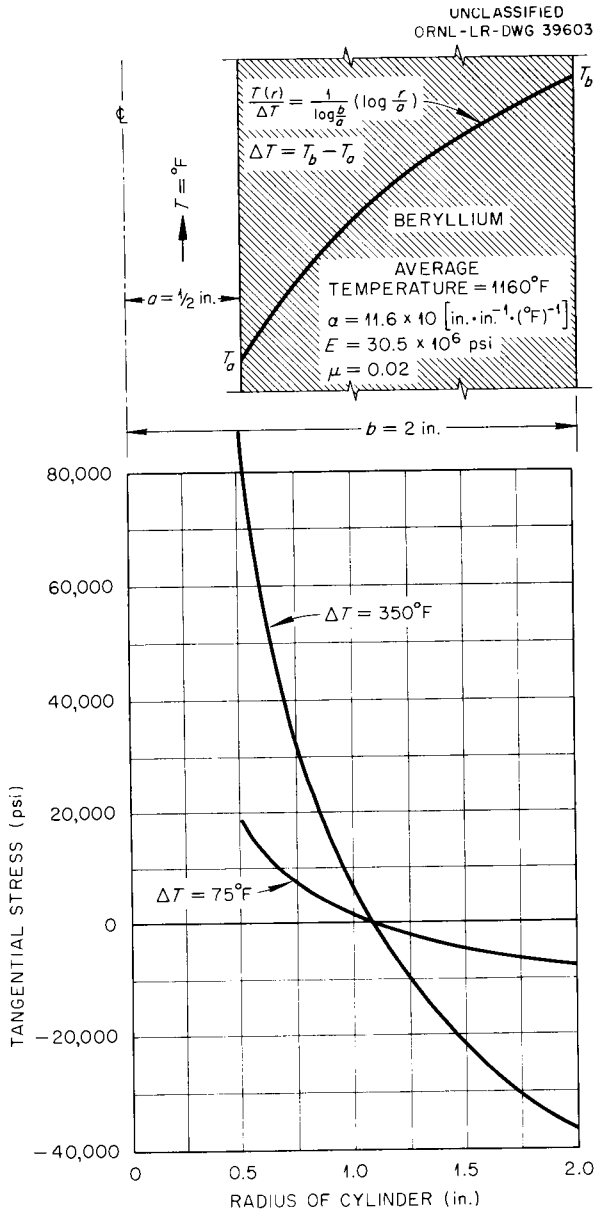

Fig. 5. Tangential Thermal Stress in a Beryllium Cylinder with a Concentric Hole.

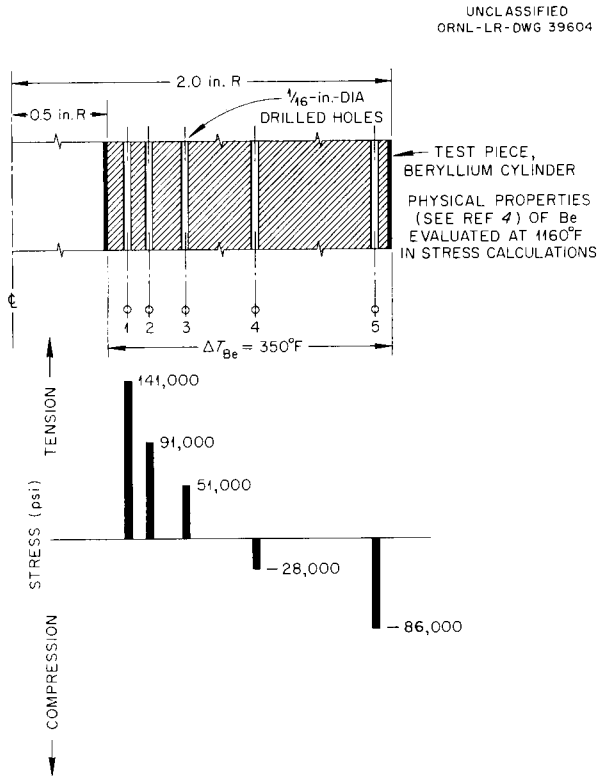

Fig. 6. Estimated Maximum Tangential Stress at Hole Boundaries in Test Piece.

Liquid sodium was used as the heat transfer medium in the test piece, which was thermally cycled at $\frac{1}{2}$-hr intervals between the temperature gradient condition and the isothermal condition so that cyclic thermal stresses would result. An idealized diagram of the desired thermal cycle is shown in Fig. 7.

The experimental arrangement used is illustrated in Fig. 8. The inner and outer cylindrical surfaces of the specimen were held at the desired temperatures by exposing them to the flowing temperature-controlled sodium.

The test specimen was enclosed in an Inconel housing (Fig. 4), which was welded into a conventional, electrically heated loop of the type used for corrosion testing (Figs. 8 and 9). Sodium from the cooling coil was directed axially through the large central hole in the test specimen, thence through the heater, around the periphery of the

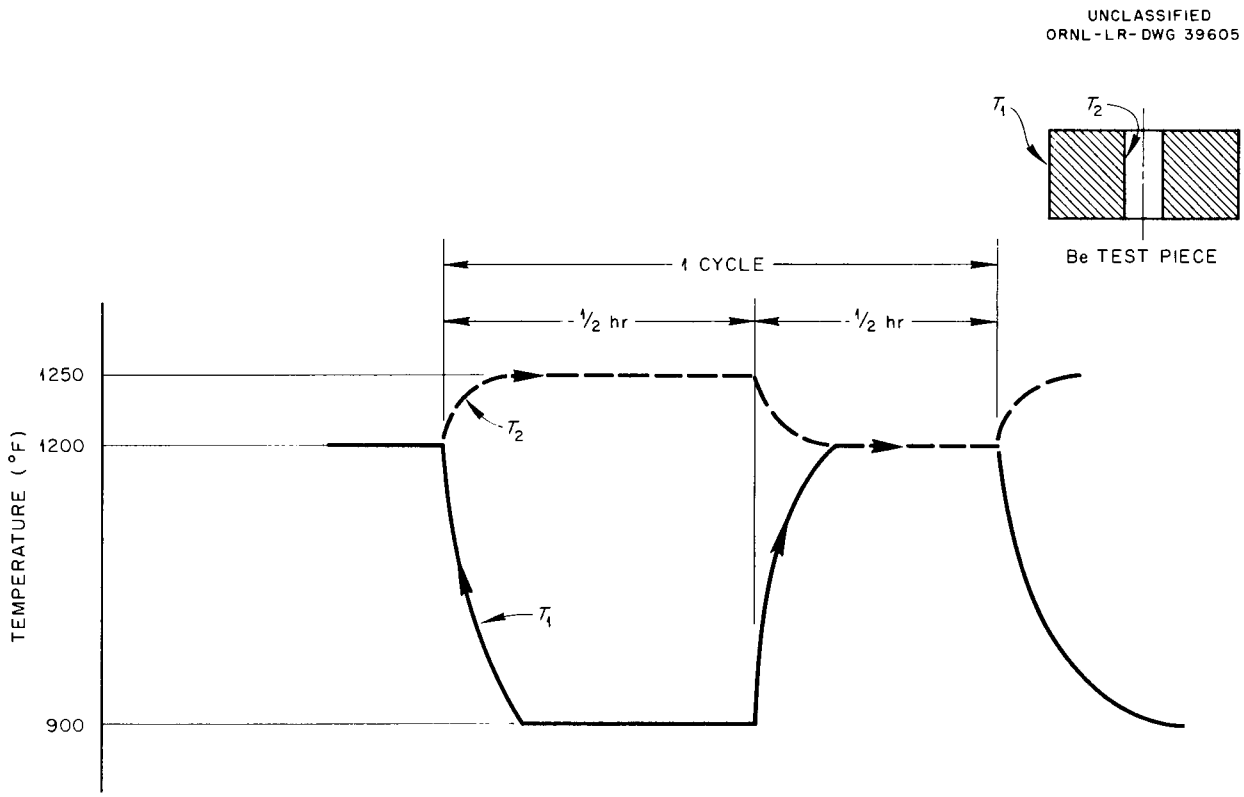

Fig. 7. Beryllium Thermal-Cycling Test Temperatures vs Time.

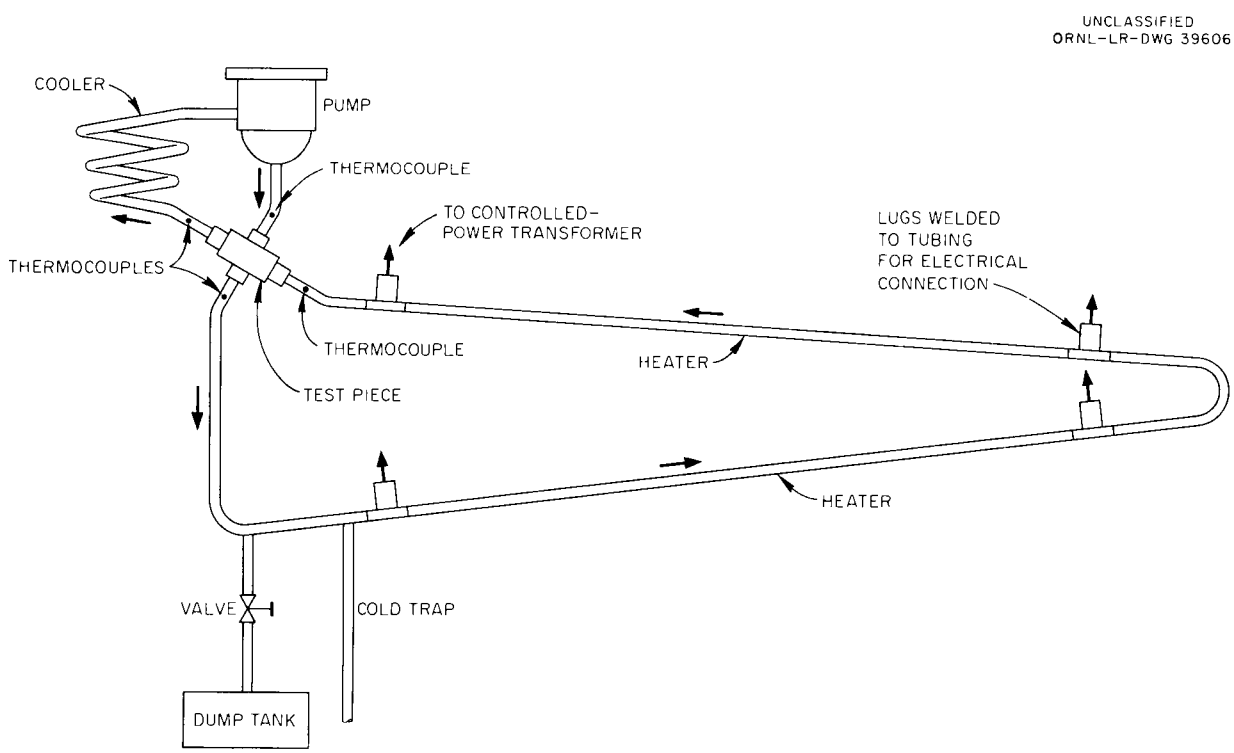

Fig. 8. Beryllium Thermal-Cycling Test Loop.

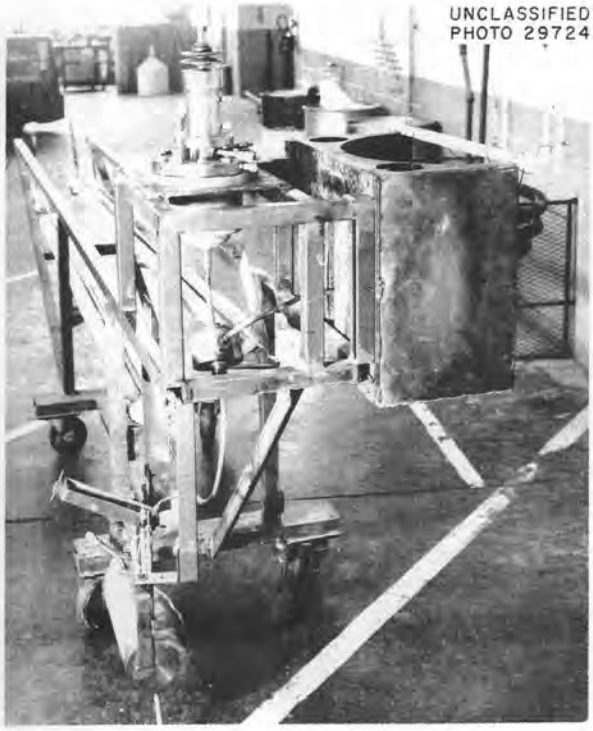

Fig. 9. Beryllium Thermal-Cycling Test Piece and Housing Installed in Test Loop.

specimen, and back to the cooling coil. The axial clearances between the ends of the specimen and its housing were minimized to reduce leakage across the end faces. Unfortunately, this was not entirely successful.

The box which housed the cooling coil was closed and heated during the isothermal part of the cycle in order to reduce radiation losses from the coil. Sodium temperatures were measured by thermocouples installed near the inlets and outlets to the test piece. A magnetic flowmeter was used to measure sodium flow.

TEST PROCEDURE AND TEST HISTORY

The loop was purged with helium when it had been assembled, and all equipment was checked. The loop was then preheated to 450°F and filled with sodium. The sodium flow was then established at 3 gpm, and the system was adjusted for isothermal operation at 1200°F. The preheaters were utilized to obtain as nearly isothermal operation as possible at the test piece. When the most nearly isothermal conditions had been obtained, the control settings were marked to facilitate the return to isothermal operation.

After ½ hr of isothermal operation, a temperature gradient was established by using a procedure similar to that described above. The operating temperatures were regulated in an effort to maintain the difference between the average hot stream temperature and the average cold stream temperature at 350°F, as indicated in Fig. 7.

The temperature history of the beryllium during the test is shown in Fig. 10, and the average hot and cold sodium temperatures during the test are shown in Fig. 11. The temperature changes experienced by both the hot and cold streams in passing through the test piece were greater than calculated. These are attributed to bypass leakage across the end faces of the specimen (Appendix C). Apparently the 0.004-in. maximum allowable clearance between the end face and housing was too large.

Completely isothermal operation was not obtained because it was impossible to reduce heat losses in the cooling coil to zero. During isothermal operation with the cooling coil at 1200°F, radiation and convection losses were sufficient to produce an inside-to-outside temperature difference of from 40 to 75°F in the test piece. This temperature difference reduced the amplitudes of the cyclic stresses or strains.

Transformer capacity was inadequate as originally designed. This was corrected at 140 cycles and permitted increasing the hot-side temperatures to the required average (see Figs. 10 and 11).

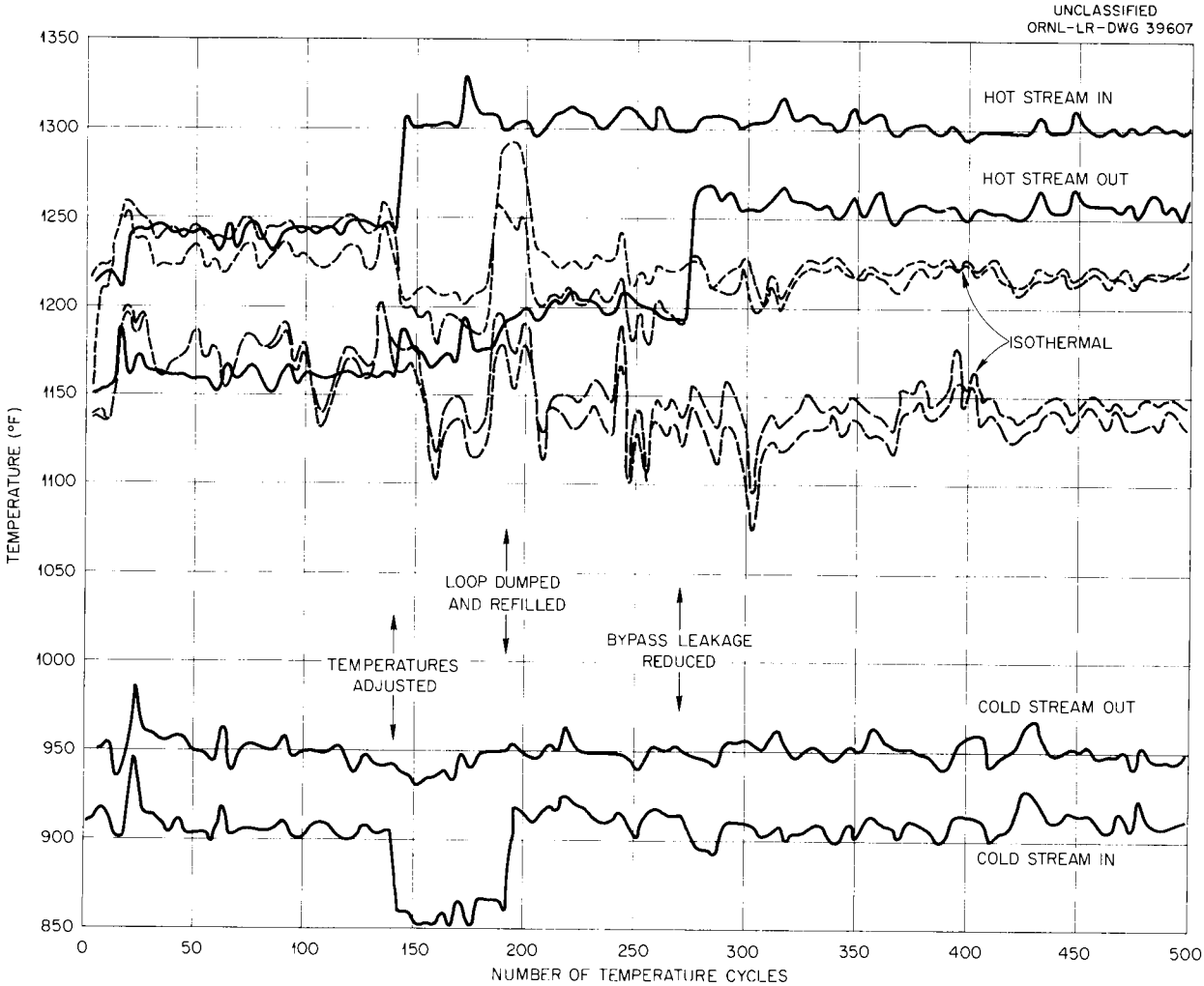

Fig. 10. Temperature History During Beryllium Thermal-Cycling Test.

Sodium oxide plugging required an increase in pump speed to maintain the flow. The effect of plugging became worse, particularly during operation with a temperature gradient, and, at the end of 185 cycles, the oxide-contaminated sodium in the loop was replaced with clean sodium.

During the drain and refill operation, failure of the bellows in the valve between the loop and the dump tank resulted in a minor fire which required the replacement of a few feet of tubing in the loop. A stagnant cold trap consisting of a vertical dead-ended tube (Fig. 8) in the coldest part of the loop was added to trap sodium oxide.

TEST RESULTS

The beryllium cylinder was found after the test to have extensive cracks (Fig. 12). All cracks were radial, and all passed through the small holes near the outer edge. It is reasonable to assume that this outer row of holes served as the origin for these radial cracks. Only one crack progressed completely through to the inner hole. It was approximately $\frac{1}{32}$ in. wide at the outer periphery, and it showed that the predominating stress at the outside surface of the cylinder was a circumferential tensile stress.

Surface discoloration and sodium oxide deposits on the transverse faces of the cylinder and on the Inconel housing (Fig. 12) indicate that the flow of sodium between the inner and outer streams was significant in the region of this large crack (Appendix C). Two possibilities are open for consideration: (1) the leakage flow followed the development of the radial crack or (2) the leakage

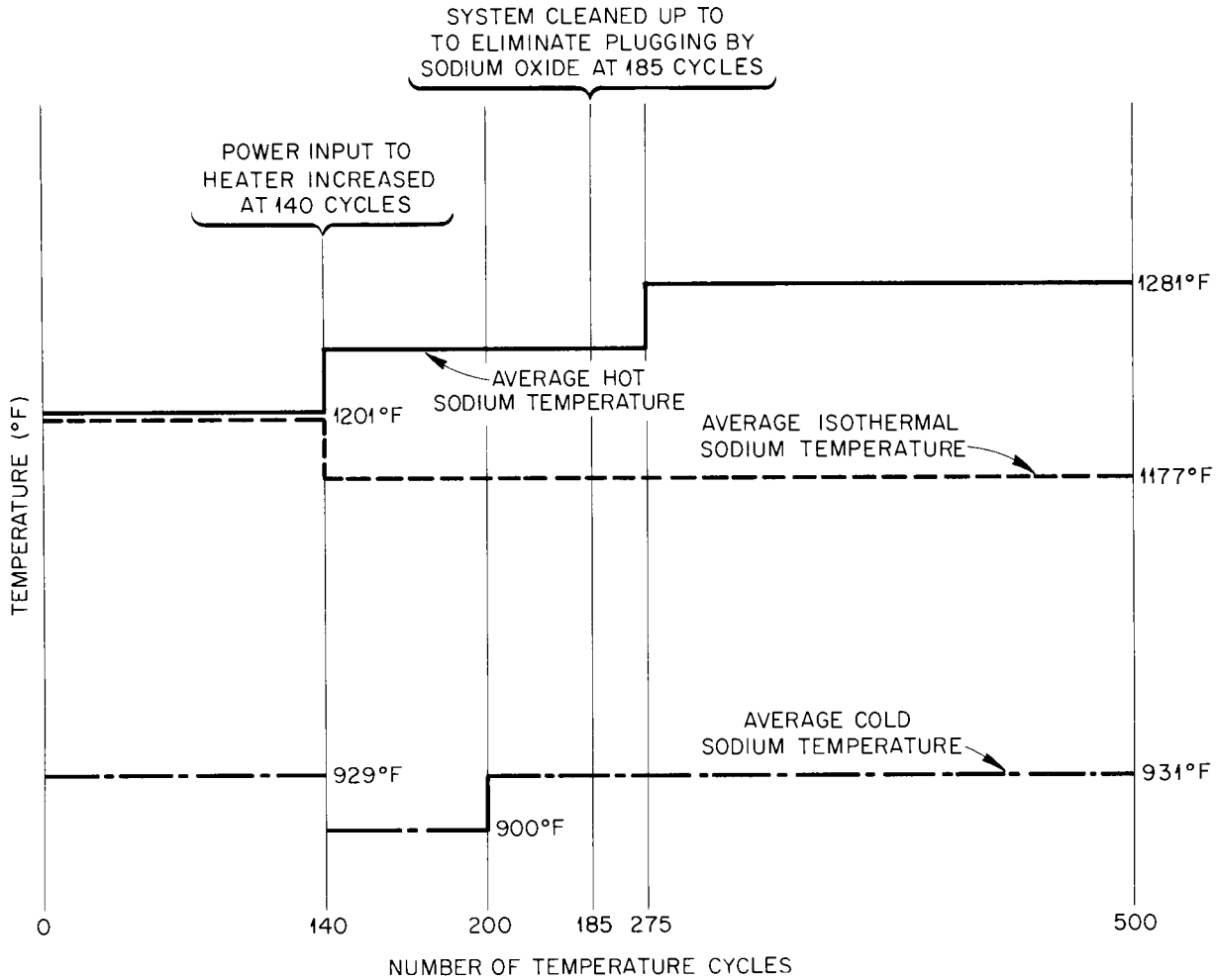

Fig. 11. Average Sodium Temperatures During Beryllium Thermal-Cycling Test.

flow path existed from the start of the test. If the latter is true, it is reasonable to conclude that leakage sodium altered the temperature gradients, produced stresses considerably higher than intended, and thus promoted the progression of the large crack to the central hole.

It can also be hypothesized that this large crack developed early in the test and progressed rapidly. If so, its existence altered the geometry of the test specimen and allowed circumferential bending; that is, the radial crack reduced the connectivity of a multiply connected region. This situation has not been analyzed, and, until an analysis has been conducted, no conclusions will be drawn. The remaining cracks terminated in the region of the average radius of the cylinder. This was logical, since the region of the average radius was the zero stress region of the cylinder (Fig. 5).

The tangential stress distribution curve (Fig. 5) indicates that it is more likely that the radial cracks would originate at the inner periphery, where the stresses are tensile and have the highest absolute value during temperature-gradient operation. However, if the stress relaxation times at test temperatures are equal to or less than the cycle time of ½ hr, strain reversal will occur during the shift to isothermal operation. The qualitative sketch of stress vs time (Fig. 13)

Fig. 12. Beryllium Test Piece and Housing After Thermal-Cycling Test.

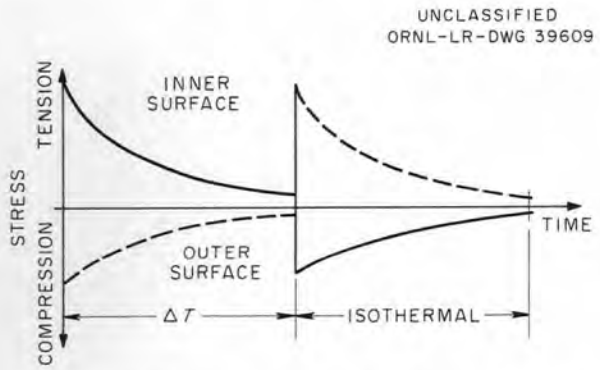

Fig. 13. Qualitative Sketch of Stress vs Time for a Typical Cycle.

illustrates stress reversals produced at the onset of isothermal temperature conditions in the test specimen by virtue of the stress relaxation which takes place during temperature-gradient operation. If it is assumed that stress relaxation[4] is virtually complete at the end of temperature-gradient operation and if during isothermal operation stress reversals essentially equal in magnitude to the stresses initially imposed by the temperature gradient take place, it may be seen that the tensile stress at the outer surface is of the same magnitude as that at the inner surface. In addition, the temperature at which the outer surface is exposed to this tensile stress is higher by approximately 300° F than that at the inner surface. The yield point of beryllium is reduced by a factor of 2 to 3 as the temperature is increased from 900 to 1200° F, whereas the other physical properties[5] contributing to thermal stress are not changed drastically. Thus it is more likely that the failure will originate at the weaker outer surface during the isothermal portion of a cycle.

CONCLUSIONS

The cracks were as anticipated in both location and orientation. The stresses imposed by the test conditions were severe, more so, perhaps, than warranted by the application the test was intended to simulate. Whereas the range of stresses experienced by the specimen was very high, it should be noted that the number of cycles (500) was relatively low. This small number of cycles was ample when compared with the 30 cycles planned for the ART operating program but wholly inadequate if applied to reactor components whose life expectancy is measured in years rather than hours.

Quantitative results cannot be obtained from a single test. In the absence of reliable strain-cycling data, designers should treat beryllium as being extremely sensitive to thermally induced strain cycling, particularly in the presence of stress-raising discontinuities.

In general, data on the physical properties and thermal behavior of beryllium under load are meager; in the area of thermally induced strain cycling, data are virtually nonexistent. Assembling these data must precede the selection of beryllium as an acceptable reactor material at elevated temperatures.

---

[4] Fig. 43, ref (5), indicates a creep of 0.002 in./in. at 1200° F during $\frac{1}{2}$ hr at a stress of 4570 psi.

[5] The thermal stress (Appendix B) is directly proportional to the quantity $\alpha E/(1-\mu)$. This quantity does not undergo any significant change in the temperature range from 900 to 1200° F.

This test demonstrated a method which, with some modifications, can be used to obtain such information. Suggested modifications are listed below:

1. Increase the length-to-diameter ratio of the sample in order to approximate more closely the infinite cylinder model which was used to calculate stresses. The infinite cylinder model assumes that the end faces remain plane before and after application of a radial temperature gradient. A test specimen having a length equal to the radius does not fulfill these conditions, and the stress calculations predicted on the infinite cylinder model are somewhat in error.
2. Reduce the sodium leakage from the outer to the inner annulus by adding labyrinth seals on the end faces. These labyrinths should be located at or near the zero thermal stress radius of the sample.
3. Reduce the fluid pressure drop between outer and inner annuli and thus reduce leakage flow.
4. Increase the sodium flow rate to reduce the temperature rise (and drop) in the sodium produced by heat transfer. This will reduce the asymmetrical temperature gradients in the sample.
5. Design the sample housing to permit easy inspection of the sample at periodic intervals. This is easily recommended, but its attainment in practice may be extremely difficult.

Appendix A

HEAT TRANSFER IN TEST PIECE

Nomenclature

ΔT	Temperature drop, °F
ΔT_{Na}	Bulk temperature change in sodium due to heat addition or removal
u	Fluid velocity, ft/hr
ρ	Fluid density, lb/ft^3
C_p	Specific heat at constant pressure, Btu·lb^{-1}·(°F)$^{-1}$
k	Thermal conductivity, Btu·hr^{-1}·ft^{-2}·(°F/ft)$^{-1}$
h	Film coefficient of heat transfer, Btu·hr^{-1}·ft^{-2}·(°F)$^{-1}$
A	Surface area providing heat transfer, ft^2
R	Thermal resistance, °F/(Btu/hr)
q	Heat transferred, Btu/hr
D_e	Equivalent diameter, ft
a	Inner radius, ft
b	Outer radius, ft
L	Thickness, ft

Subscripts i, Be, and o refer to the inner sodium film, the beryllium test piece, and the outer sodium film, respectively.

Temperature Calculations

The total temperature drop from the outer to the inner sodium annulus is divided into three parts:

1. temperature drop across outer sodium film, ΔT_o,
2. temperature drop across the beryllium sample, ΔT_{Be},
3. temperature drop across the inner sodium film, ΔT_i.

The temperature drops were computed from the familiar relation

$$\Delta T = qR \quad . \tag{A-1}$$

Applying Eq. (A-1) to the system shown in Fig. 4 gives

$$\Delta T_o = qR_o = \frac{q}{A_o h_o} \quad , \tag{A-2a}$$

$$\Delta T_{Be} = qR_{Be} = \frac{q \log (b/a)}{2\pi L k} \quad , \tag{A-2b}$$

$$\Delta T_i = qR_i = \frac{q}{A_i h_i} \quad . \tag{A-2c}$$

The heat transferred, q, can be determined from Eq. (A-2b) by inserting the specified value of ΔT_{Be}. Film coefficients h_o and h_i are calculated from the well-known Lyon-Martinelli (6) equation:

$$\frac{hD_e}{k} = 7 + 0.025\left(\frac{D_e u C_p}{k}\right)^{0.8} . \tag{A-3}$$

The thermal conductivity of beryllium (6) is given as a function of temperature in Fig. A.1. Table A.1 lists the pertinent physical properties of sodium (7) and the results of applying Eqs. (A-1), (A-2), and (A-3) to the test setup at a sodium flow rate of 3 gpm and a total temperature drop, ΔT, of 350° F.

It is apparent that the film temperature drops contribute little to the over-all temperature difference between the hot and cold sodium streams. It is also apparent that the major contribution to the inner and outer film coefficients is from the constant term, 7, in Eq. (A-3); that is, the film temperature drops will be a constant percentage of the over-all temperature differential across the test piece. This simplifies the determination of the actual temperature gradient, ΔT_{Be}, across the test piece in terms of test data. Referring to the data in Table A.1, it may be seen that ΔT_{Be} is 96% of the hot to cold sodium temperature difference; that is, this value of ΔT_{Be} can be applied to all test data without serious error. The calculated temperature profile in the test chamber for an assumed total ΔT of 350° F is shown in Fig. A.2.

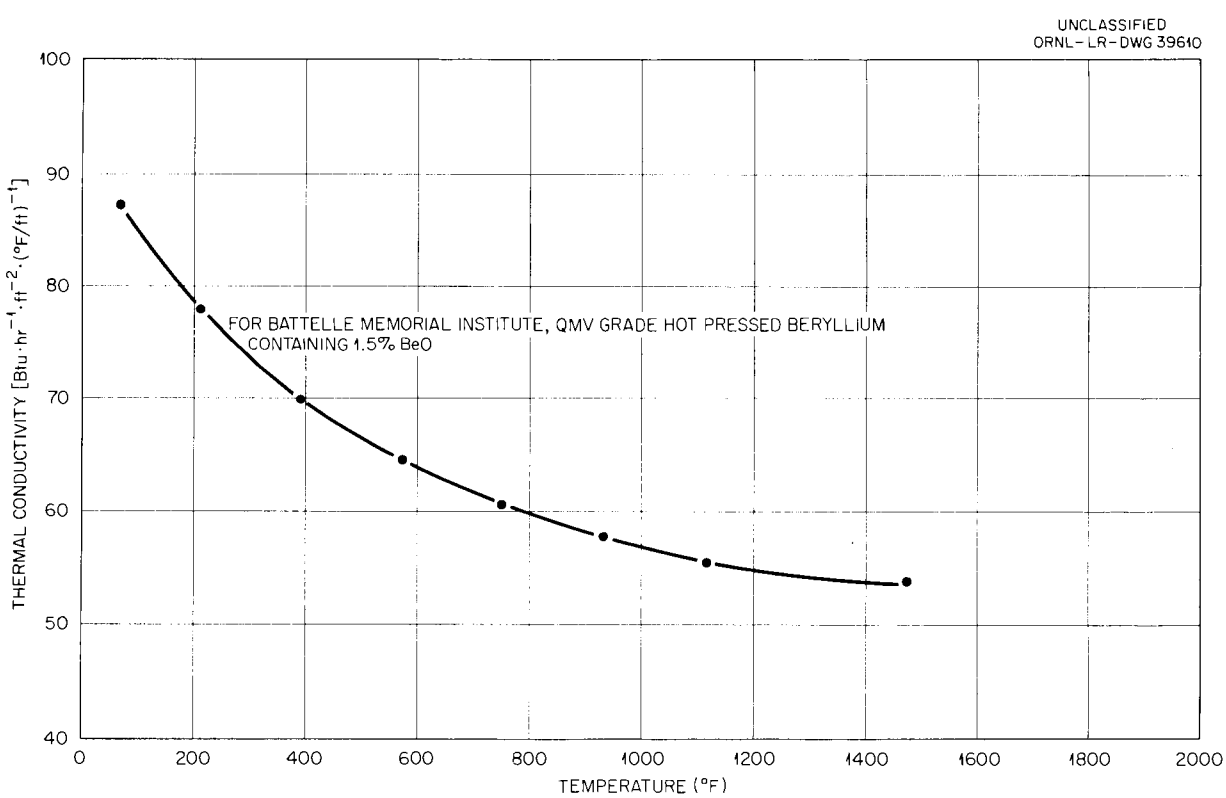

Fig. A.1. Thermal Conductivity of Beryllium vs Temperature.

Table A.1. Pertinent Physical Properties of Sodium

Quantity	Inner Annulus	Outer Annulus
u	56,800 ft/hr	13,590 ft/hr
k/C_p	2.60 $lb \cdot hr^{-1} \cdot ft^{-1}$ (at 900° F)	2.50 $lb \cdot hr^{-1} \cdot ft^{-1}$ (at 1200° F)
k	39.0 $Btu \cdot hr^{-1} \cdot ft^{-2} \cdot (°F/ft)^{-1}$ (at 900° F)	35.0 $Btu \cdot hr^{-1} \cdot ft^{-2} \cdot (°F/ft)^{-1}$ (at 1200° F)
D_e	0.01085 ft	0.01033 ft
A	0.0437 ft^2	0.1745 ft^2
hD_e/k	7.00 + 2.05 = 9.05	7.00 + 0.81 = 7.81
h	32,600 $Btu \cdot hr^{-1} \cdot ft^{-2} \cdot (°F)^{-1}$	26,800 $Btu \cdot hr^{-1} \cdot ft^{-2} \cdot (°F)^{-1}$
ΔT_{film}	10° F	3° F
q	14,100 Btu (at ΔT_{Be} = 337° F)	14,100 Btu
$\Delta T_{bulk\ Na}$	77° F	−77° F

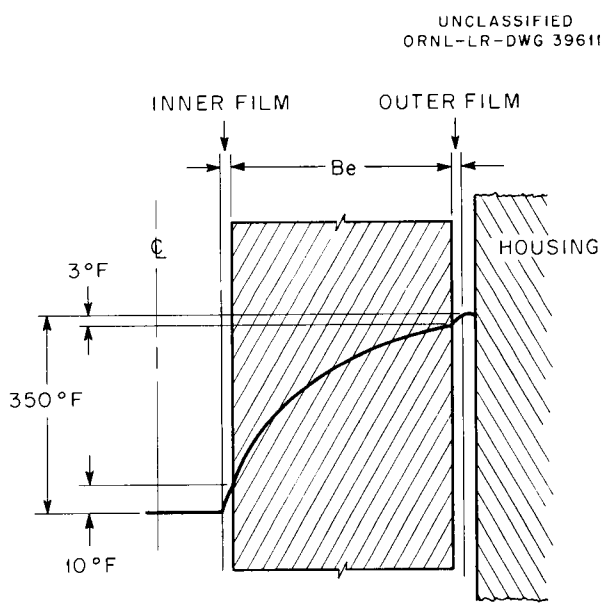

Fig. A.2. Calculated Temperature Profile in Test Chamber.

Appendix B

STRESS CALCULATIONS

Nomenclature

σ_θ	Tangential thermal stress, psi
E	Modulus of elasticity, psi
α	Coefficient of thermal expansion, in.•in.$^{-1}$•(°F)$^{-1}$
μ	Poisson's ratio
a	Inner radius, in.
b	Outer radius, in.
r	Radius, in.
$T(r)$	Temperature as a function of radius r, °F
T_a	Temperature at inner radius, °F
T_b	Temperature at outer radius, °F
ΔT_{Be}	Temperature difference from outer surface to inner surface, °F:

$$\Delta T_{Be} = T_b - T_a$$

Tangential Stress Calculations in Beryllium Test Piece

The general expression for tangential stress, σ_θ, in a long circular cylinder with a concentric hole (*4*) is

$$\sigma_\theta = \frac{\alpha E}{1-\mu}\,\frac{1}{r^2}\left[\frac{r^2+a^2}{b^2-a^2}\int_a^b r\,T(r)\,dr + \int_a^r r\,T(r)\,dr - r^2T(r)\right] . \tag{B-1}$$

In a long cylinder having uniform values of α, E, and μ and experiencing steady-state inward radial heat flow, the temperature distribution is given by

$$T(r) = T_a + \frac{\Delta T_{Be}}{\log\,(b/a)}\log\frac{r}{a} . \tag{B-2}$$

Substituting the temperature from Eq. (B-2) into Eq. (B-1):

$$\sigma_\theta = \frac{\alpha E\,\Delta T_{Be}}{1-\mu}\,\frac{1}{\log\,(b/a)}\left[\frac{a^2}{b^2-a^2}\left(1+\frac{b^2}{r^2}\right)\log\frac{b}{a} + \log\frac{b}{r} - 1\right] . \tag{B-3}$$

Stresses calculated by Eq. (B-3) for $\Delta T_{Be} = +350°$F and $\Delta T_{Be} = +75°$F are given in Fig. 5. The values $a = 0.50$ in. and $b = 2.00$ in., along with the physical property data of Table B.1, including the data of Fig. B.1, were used. The data in the table are for beryllium at 1160°F.

Tangential Stress Calculations in Beryllium Reflector

The largest radial temperature gradient in the reflector is located 10 in. above the equator ($Z = 10$, Fig. 1). The temperature is linear with respect to the radius, and thus

$$T(r) = T_a + \Delta T_{Be}\,\frac{(r-a)}{(b-a)} . \tag{B-4}$$

Table B.1. Physical Property Data for Beryllium at 1160°F

Quantity	Value	Reference
E	30.5×10^6 psi	(5)
α	11.6×10^{-6} in.·in.$^{-1}$·(°F)$^{-1}$	Fig. B.1
μ	0.02	(9)

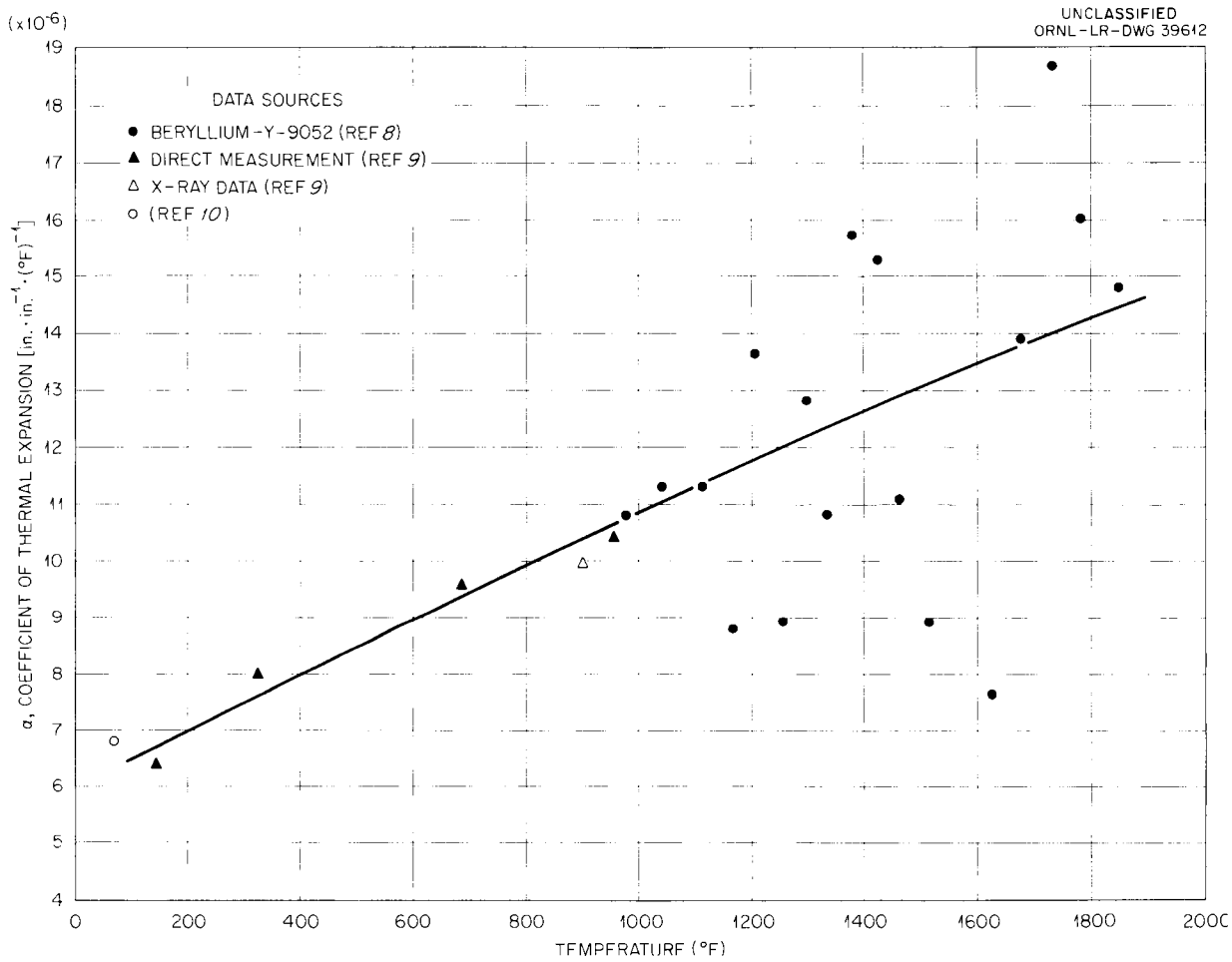

Fig. B.1. Coefficient of Thermal Expansion for Beryllium.

The substitution of the temperature from Eq. (B-4) into Eq. (B-1) produces[1]

$$\sigma_\theta(r) = \frac{\alpha E \Delta T_{Be}}{1-\mu} \frac{1}{3r^2(b^2-a^2)} [r^2(b^2+ab+a^2) - 2r^3(b+a) + a^2 b^2] \cdot \tag{B-5}$$

Inserting the values $a = 8$ in., $b = 19$ in., $\Delta T_{Be} = 180°$ F, and using the physical properties from Table B.1, Eqs. (B-4) and (B-5) become:

$$T(r) = 1070 + 180 \frac{(r-8)}{11} , \tag{B-4a}$$

$$\sigma_\theta(r) = 65{,}000 \left(0.648 - 0.061\, r + \frac{25.930}{r^2} \right) . \tag{B-5a}$$

The stresses so calculated are given on Fig. 2.

---

[1] The constant T_a does not produce any thermal stress and may be omitted in making this substitution.

Appendix C

FLOW RESISTANCE CALCULATIONS

The results of flow resistance calculations, expressed in equivalent lengths of 0.460-in.-ID tubing, are diagramed in Fig. C.1. As may be seen, the resistance of the long length, 29 ft, of heater tubing offers considerable incentive for the cold sodium to bypass the heater by flowing radially across the transverse faces of the test piece. The design clearance (axial) between the test piece and its housing was 0.002 to 0.004 in. in order that the resistance to bypass flow be as large as possible.

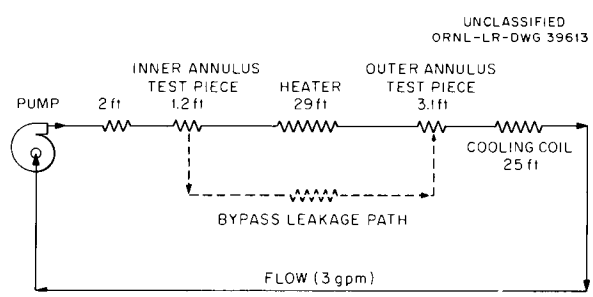

Fig. C.1. Calculated Flow Resistances in Test System.

REFERENCES

(1) D. L. Platus, *Beryllium Cycling Test*, ORNL CF-57-2-81 (Feb. 20, 1957).

(2) D. L. Platus, D. M. Miller, and R. V. Meghreblian, *ART Reflector Temperature Distribution*, ORNL-2425 (Nov. 2, 1957).

(3) R. V. Meghreblian *et al.*, *ANP Quar. Prog. Rep. Sept. 30, 1957*, ORNL-2387, p 72.

(4) S. Timoshenko and J. N. Goodier, *Theory of Elasticity*, 2d ed., pp 78, 408, McGraw-Hill, New York, 1951.

(5) R. G. O'Rourke *et al.*, *Mechanical Properties of Reactor-Grade Beryllium at Elevated Temperatures*, COO-312 (August 1956).

(6) Private communication with R. V. Meghreblian.

(7) C. B. Jackson (Editor-in-Chief), *Liquid Metals Handbook. Sodium-NaK Supplement*, TID-5277, pp 39, 73 (July 1, 1955).

(8) I. B. Fieldhouse, letter to Commander, Wright Air Development Center (Attn.: Mr. H. Marcus, WCRTY-3) regarding Armour Research Foundation Contract No. AF 33 (616)-3701 (March 26, 1957).

(9) *The Reactor Handbook*, vol 3, "Materials," AECD-3647, p 60 (March 1955).

(10) C. A. Hampel (ed.), *Rare Metals Handbook*, p 31, Reinhold, New York, 1954.

INTERNAL DISTRIBUTION

1. M. Bender
2. D. S. Billington
3. F. F. Blankenship
4. E. P. Blizard
5. A. L. Boch
6. C. J. Borkowski
7. G. E. Boyd
8. E. J. Breeding
9. R. B. Briggs
10. D. W. Cardwell
11. C. E. Center (K-25)
12. R. H. Chapman
13. R. A. Charpie
14. R. D. Cheverton
15. B. Y. Cotton
16. F. L. Culler
17. D. A. Douglas
18. L. B. Emlet (K-25)
19. D. E. Ferguson
20. J. Foster
21. A. P. Fraas
22. J. H. Frye, Jr.
23. B. L. Greenstreet
24. W. R. Grimes
25. E. Guth
26. C. S. Harrill
27. H. W. Hoffman
28. A. Hollaender
29. A. S. Householder
30. W. H. Jordan
31. P. R. Kasten
32. G. W. Keilholtz
33. C. P. Keim
34. M. T. Kelley
35. W. H. Kelley
36. B. W. Kinyon
37. J. A. Lane
38. R. S. Livingston
39. H. G. MacPherson
40. W. D. Manly
41. R. L. Maxwell
42. J. R. McNally
43. J. T. Meador
44. A. J. Miller
45. S. E. Moore
46. K. Z. Morgan
47. J. P. Murray (Y-12)
48. M. L. Nelson
49. A. M. Perry
50. P. M. Reyling
51. G. C. Robinson
52. G. Samuels
53. H. W. Savage
54. A. W. Savolainen
55. W. L. Scott
56. H. E. Seagren
57. E. D. Shipley
58. M. J. Skinner
59. A. H. Snell
60. F. J. Stanek
61. J. A. Swartout
62. J. R. Tallackson
63. E. H. Taylor
64. A. M. Weinberg
65. G. C. Williams
66. C. E. Winters
67. F. J. Witt
68. Biology Library
69. Health Physics Library
70. Reactor Experimental Engineering Library

71–72. Central Research Library
73–92. Laboratory Records Department
93. Laboratory Records, ORNL R.C.
94–98. ORNL – Y-12 Technical Library, Document Reference Section

EXTERNAL DISTRIBUTION

99. Division of Research and Development, AEC, ORO

100–660. Given distribution as shown in TID-4500 (14th ed.) under Metallurgy and Ceramics category (75 copies – OTS)